Porous granules by freeze granulation of Pickering emulsions stabilized with halloysite particles

M. Ouadaker, X. Jiang, P. Bowen, M. Bienia, C. Pagnoux, A. Aimable

1 **Porous granules by freeze granulation of Pickering emulsions**

2 **stabilized with halloysite particles**

3 M. Ouadaker[(1)], X. Jiang[(2)], P. Bowen[(2)], M. Bienia[(1)], C. Pagnoux[(1)], A. Aimable[(1)*]

4 (1) Univ. Limoges, CNRS, IRCER, UMR 7315, F-87000 Limoges, France

5 (2) Laboratory of Construction Materials (LMC), Swiss Federal Institute of Technology EPFL,
6 1015, Lausanne, Switzerland
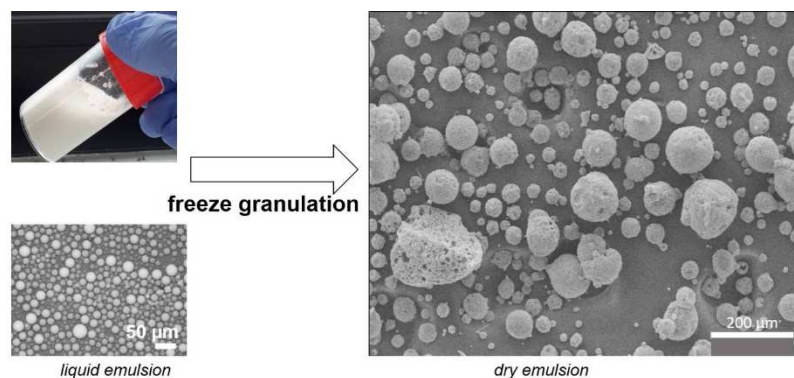
7

8 * Corresponding author:
9 Anne Aimable
10 E-mail : anne.aimable@unilim.fr
11 Phone : +33 (0) 587 50 23 68
12 Fax : +33 (0) 587 50 23 04
13

14 **Graphical abstract**

15

16

17 **Abstract**

18 Pickering emulsions stabilized with a natural silicate mineral, halloysite, were dried by freeze

19 granulation in order to prepare porous granules. Different formulations were studied, by varying

20 the pH of the suspension, the ionic strength and with the addition of organic binders (poly(vinyl

21 alcohol) (PVA) and poly(ethylene glycol) (PEG)). To get a better understanding and control on

22 the process the objective was to correlate the formulation and the emulsion behavior to the

23 morphology and size of the granules. This study highlights the predominant role of electrostatic

24 interactions on the emulsions. Their stability is improved if the dispersion of solid particles in

25 the continuous phase is relatively limited, with medium zeta potential absolute values. Freeze

26 granulation of emulsions prepared at different ionic strength and pH led to similar granules,

1

with an internal porosity attributed to the low solid fraction. The addition of organic additives PVA and PEG led to a better conservation of the structure, with fewer broken fragments and a larger porosity, attributed to a higher cohesion of these emulsions during the spray freezing and the lyophilisation steps.

Keywords

Pickering emulsion; freeze granulation; lyophilisation; halloysite; porosity; rheology

1- Introduction

Pickering emulsions are emulsions stabilized by solid particles adsorbing at the liquid/liquid interface [1]. They were first described by Ramsden [2] and Pickering [3]. They are employed in many different fields, such as cosmetics, paints, food industry, or coal treatments. They present a very long shelf life and a strong resistance to coalescence attributed to a non-reversible attachment of solid particles at the oil-water interface. This mechanism was extensively supported by a theoretical approach and thermodynamic calculations, described in many publications [4][5][6][7]. The type of emulsion is determined by the particle wettability at the oil-water interface: hydrophilic particles lead to the dispersion of the oil phase in the aqueous medium (O/W), whereas hydrophobic particles to the dispersion of the aqueous phase (W/O) [8]. Surface properties are generally modified, either by organic species adsorption or chemical grafting, to enhance emulsion stability [9][10][11][12][13]. However stabilization of emulsions without additives is a real challenge, especially for cosmetic and food applications, where lowering the amount of chemicals is of great benefit for the health of the consumers. The use of clay minerals such as montmorillonite [14], mica [15], hectorite and bentonite [16], or laponite [17] was reported in the literature. The stabilization of Pickering emulsions without surface modification is possible because their chemistry and the layer structure allow them to have amphiphilic properties [18]. In that context, clays offer a great opportunity for the development of surfactant-free emulsions. Moreover they are readily available, cheap and natural resources.

In a previous study, we compared kaolin, halloysite and palygorskite as Pickering emulsion stabilizer [19]. All three phyllosilicates led to stable emulsions at high solid contents (15 wt.% equal to 5.0 vol.% in the aqueous phase) without any surface modification. They showed different rheological behaviors, halloysite leading to the highest cohesion of the emulsion, which was attributed to its higher specific surface area.

60 In the present study the aim was to prepare porous granules from Pickering emulsions of
61 halloysite via freeze granulation. This process consists of an atomization into small droplets of
62 a suspension or an emulsion through a spraying nozzle [20]. Droplets are sprayed into liquid
63 nitrogen under stirring and are instantly frozen. The resulting frozen granules are recovered
64 and subsequently freeze-dried under vacuum to sublimate the ice they contain and yield a dry
65 granulated powder. Compared to the spray-drying process [21][22], freeze granulation leads
66 to a better control of granule density and a higher homogeneity. Indeed, droplet freezing is a
67 fast process, and lyophilisation prevents shrinkage and deformations generally observed
68 during the drying step (such as the doughnut effect). This technology presents the great
69 advantage to preserve the structure and homogeneity of the particles in suspension [23]. It is
70 suitable for the preparation of fine powders, re-dispersible formulations, nanomaterials, drug
71 delivery systems, etc... Organic compounds, pharmaceutical products or other heat sensitive
72 materials benefit from this low temperature and low pressure process. Technical ceramics
73 such as transparent ceramics [24][25], MOX fuels [26] or non-oxide ceramics [27][28][29] have
74 also been prepared with high performances.

75 Freeze granulation was chosen for its ability to retain the structure of the slurry. The aim was
76 to investigate if an O/W Pickering emulsion could lead to the formation of macroporous
77 granules made of ceramic materials after elimination of the liquid phases. If there are many
78 papers published on processing routes based on Pickering emulsions, most of them deal with
79 organic materials. Macroporous ceramic materials are obtained by processing routes generally
80 classified into replica, sacrificial template, and direct foaming methods [30]. However some
81 groups have reported on particle-stabilized emulsions as templates for the fabrication of
82 porous materials [10][31][32]. More recently additive manufacturing such as extrusion-based
83 3D printing also succeeded in the fabrication of hierarchical porous materials, leading to very
84 well-designed and complex geometries [33][34][35]. A large range of applications exist for such
85 macroporous ceramic materials such as drug delivery systems, chemical containers, or
86 catalyst supports.

87 Therefore different formulations of emulsions were studied, by varying the pH of the
88 suspension, the ionic strength and with the addition of organic binders (poly(vinyl alcohol)
89 (PVA) and poly(ethylene glycol) (PEG)). Through this study we tried to get a better
90 understanding and control on the process by making correlations between the formulation, the
91 emulsion behavior and the morphology and size of the materials obtained by freeze
92 granulation.

93

94

2- Experimental section

2.1 Raw materials

Halloysite powder is provided by Imerys Ceramics under the name Premium NZCC. This clay is a phyllosilicate with the formula $Al_2Si_2O_5(OH)_4 \cdot nH_2O$, n being comprised between 0 and 2. Halloysite is a dioctahedral 1:1 clay mineral of the kaolin group and has a multilayer tubular structure. This structure results from the wrapping of the 1:1 clay mineral layers, driven by a mismatch in the oxygen-sharing tetrahedral and octahedral sheets in the 1:1 layer. Halloysite is chemically similar to kaolin, but the unit layers are separated by a layer of water molecules. This gives a remarkable surface chemistry of halloysite: the external surface of the tubes is composed of Si–O–Si groups, whereas the internal lumen surface consists of a gibbsite-like array of Al–OH groups [36][37][38]. This lead to different surface charges of the materials depending on the pH.

Halloysite presents an elongated tubular morphology, with a width around 100 nm and a length of 1-2 µm. The morphology of the particles is visible in the SEM image (Figure 1a), and Figure 1b shows the particle size distribution of halloysite measured by laser diffraction, which is bimodal, corresponding to the two sizes (width and length) of particles, expected for platelet like particles with such a large difference between thickness and length [39], as well as a small agglomeration of these particles.

(a)   (b)
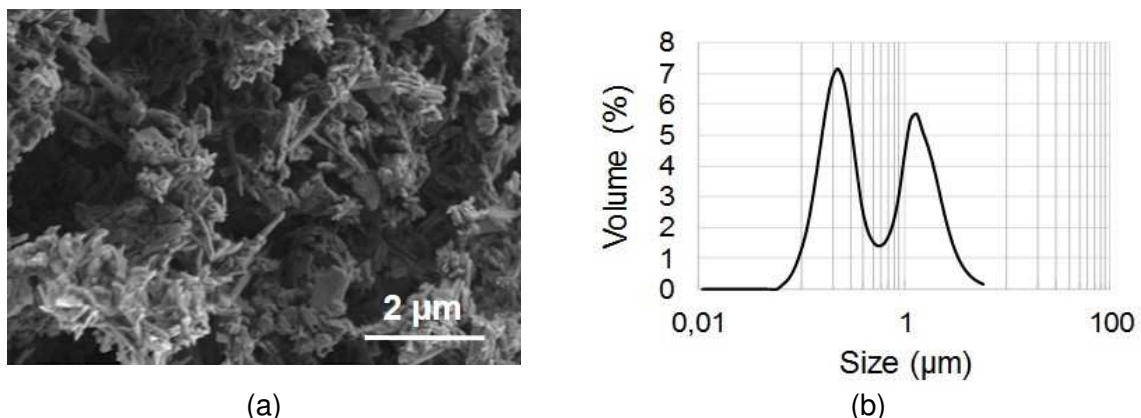
Figure 1: (a) SEM image of halloysite, (b) Particle size distribution of halloysite by laser granulometry (in diluted aqueous suspension, natural pH)

Halloysite density was taken at 2.8 g/cm^3. Halloysite was dispersed into deionized water, or NaCl solutions at different concentrations (prepared from NaCl 99%, Aldrich). Dodecane ($C_{12}H_{26}$, Sigma-Aldrich, density = 0.75 g/cm^3) was used without further treatment as the oil phase.

121 PVA (poly(vinyl alcohol), Mw = 25000g/mol) and PEG (poly(ethylene glycol), Mw = 300g/mol)

122 from Aldrich were used respectively as binder and plasticizer to increase the cohesion of the

123 final powder during the freeze granulation process.

124

2.2 Emulsion preparation procedure

126 Emulsions are obtained by mixing aqueous suspensions of halloysite with dodecane. In a

127 typical formulation, halloysite particles were introduced into the water at the volume fraction

128 5.0 vol.%. This suspension was stirred magnetically at 500 rpm during two minutes, and

129 dispersed using an ultrasonic pulsing method (3s On, 1s Off) during two minutes. Then

130 dodecane was added at a ratio R corresponding to the volume ratio of dodecane to water of

131 0.44 (defined by a previous study [19]). A high-shear stirring was applied at 19000 rpm during

132 two minutes with an Ultra-Turrax T25 homogenizer in order to form the emulsion.

133 To study the effect of the pH, NaOH (0.1M) solution was introduced into the suspension

134 (natural pH = 3.4) controlled using a pH-meter.

135 To study the effect of the ionic strength of the suspension, NaCl solutions at different known

136 concentrations were used instead of water.

137 In order to increase the cohesion of the material during the freeze granulation processing step,

138 a mixture of polymers, PVA and PEG, was also added at different concentrations. They were

139 previously diluted in water, and introduced into the suspension to the desired concentration

140 prior to the emulsification step.

141

2.3 Freeze granulation of halloysite stabilized emulsions

143 The main objective of this study was to dry Pickering emulsions of halloysite by freeze

144 granulation. This operation follows two stages: the first is spray freezing, and the second is

145 freeze drying (or lyophilization).

146 Spray freezing consists of spraying a suspension (here an emulsion) with compressed air into

147 a large volume (around 1 liter) of liquid nitrogen, in order to form granules by an instantaneous

148 freezing of the fluid droplets. The rapid freezing allows the conservation of the spherical shape

149 created by spraying through the nozzles. The freeze granulator (LS-2, PowderPro AB) is

150 equipped with a suspension flow regulating device provided with the apparatus. The atomizer

151 used was of the twin-fluid nozzle type. Both air and suspension inlets had inner diameters of 4

152 mm and the droplet spraying outlet had an inner diameter of 1 mm. The atomization gas used

153 was air. Unless otherwise stated, the atomization conditions performed were: air relative

154 pressure of 0.2 bar and suspension flow rate of 33 mL/min (suspension pumped through a

155 peristaltic pump). The rotation speed of the magnetic stirrer in the liquid nitrogen was set at

156 350 rpm. Immediately after formation, frozen granules were freeze dried in a Christ Alpha 2–4

157 LD Plus freezedrier. Freeze drying aims at removing the liquid phase present in the frozen
158 suspension or emulsion granules by sublimation. This procedure lasts about 20 hours to
159 maintain the structure of the granules after removing the liquid, under a final vacuum of 10^{-3}
160 mbar.

161

162 **2.4 Characterization techniques**

163 Zeta potential measurements were conducted on halloysite suspensions (5 vol.%) with an ESA
164 analyser (AcoustoSizer II S flow through system, Colloidal Dynamics). The zeta potential was
165 obtained from the ESA voltage data treated with the AcoustoSizer II operation software by
166 using the O'Brien relationship. Zeta potential measurements were done varying the ionic
167 strength by NaCl addition, varying pH with 1.0 mol/L sodium hydroxide addition, or with an
168 addition of PVA and PEG as aqueous solutions at the concentration 10 wt.%, with the
169 automated AcoustoSizer II pH titration system.

170 The stability, phase separation or creaming of emulsions was characterized after visual
171 observations.

172 Emulsion droplets were observed using an optical microscope Nikon Eclipse 501. A small
173 amount of freshly prepared emulsion was placed on a microscope slide, and covered after
174 ensuring that no air gap or bubbles were trapped between the sample and the cover slip.

175 Laser diffraction analysis was used to determine the droplet size distribution of emulsions
176 (Horiba LA-950), using the Fraunhofer mode. Emulsions were analysed in the liquid module,
177 whereas freeze dried granules were analysed in the dry module.

178 Emulsions were characterized using a stress-controlled rheometer ARG2 from TA Instruments.
179 The measuring geometry consisted of a 20 mm diameter upper plate and a Peltier lower plate.
180 The gap was set to 1 mm.
181 The viscous and elastic responses were investigated by dynamic oscillatory tests carried out
182 at 20 °C. The principle of this measurement is to apply a sinusoidal strain and measure the
183 corresponding stress. In this procedure the linear viscoelastic region can be detected. The
184 dynamic response between strain (γ) and stress (τ) can be described as follows:
185      $\tau = G^*\gamma$ (1)
186   where G* is the complex modulus consisting elastic (G') and viscous (G'') components.
187 The relationships are shown below and $\tan \delta$ is the loss factor which equals to G''/G':
188      $G' = G_0 \cos \delta$ (2)
189      $G'' = G_0 \sin \delta$ (3)
190 The linear viscoelastic region (LVER) is determined by oscillatory strain sweep from 10^{-4} to 0.1
191 at a fixed frequency of 1 Hz. The critical elastic modulus (G'_C) and critical strain (γ_c) are obtained

192   from the flow onset point, and the onset point allows us to calculate the cohesive energy E_c

193   using the equation below:

194           $E_C = \frac{1}{2} G'_C \gamma_C^2$ (4)

195   The cohesive energy corresponds to the elastic strength of the material, and thus could be

196   considered as a measurement of the strength of the internal structure of the emulsion; the

197   higher the cohesive energy, the more stable a system should be.

198   In order to characterize better the rheological behavior during the pumping operation, steady

199   state flow measurements were also performed. They consist of a series of creep experiments

200   with varying stress, where the equilibrium shear rate is obtained when the curve reaches a

201   linear regime. The stress was varied using the following cycle:

202   1. a pre-shear at the maximum shear stress (20 Pa),

203   2. a decreasing shear stress sweep,

204   3. an increasing shear stress sweep.

205   The morphology and size of materials obtained by freeze granulation were observed by

206   Scanning Electron Microscopy (SEM, Quanta 450 FEG) under vacuum mode (HV: 2 keV,

207   working distance: 9 mm, spot: 3.0).

208

209   **3- Results and discussion**

210

211   **3.1- Influence of pH on halloysite suspensions and emulsions**

212   Zeta potential of an halloysite suspension (concentration 5.0 vol.%) was measured as a

213   function of the pH (Figure 2). Halloysite suspension in deionized water presents a natural pH

214   value of 3.4 corresponding to a negative zeta potential value of -14 mV. By adding NaOH, the

215   pH increases and the zeta potential decreases rapidly, to attain -50 mV at pH 10, ensuring a

216   better dispersion of particles, and thus a better stability of the suspension. The typical tubular

217   morphology of halloysite is described with the Si-OH groups on the outer surface, whereas the

218   inner surfaces of the tubes present Al-OH groups [36][37][38]. Therefore the measurement

219   obtained from the Acoustosizer (which is an average zeta response) is more similar to a silica

220   material, because of its presence at the external surfaces. Moreover in the acidic pH range,

221   the inner and the outer surfaces present opposite charges, whereas at basic pH, both surfaces

222   are negative, leading to higher absolute values.

223   Emulsions were prepared with dodecane at a volume ratio R = 0.44. A stable O/W emulsion

224   was obtained at the natural pH (Figure 3(a)). Optical microscopy shows that halloysite particles

are located at the O/W interface, but also in the continuous aqueous phase (Figure 3(b)). Increasing the pH of the suspension impacted the stability of the emulsion, and creaming was rapidly observed at pH > 7.0 (Figure 3(a)). This corresponds to the transition from positive to neutral and negative surface charges of the alumina-like surfaces. It has been shown that most oil phases present negative surface charges [40][41], therefore repulsive interactions between halloysite particles and dodecane increase when pH increases, leading to the emulsion breaking. Furthermore a higher zeta potential in absolute value corresponds to a better dispersion of halloysite particles in the aqueous phase, which is not favorable for their migration at the oil/water interface. To conclude, a high negative surface charge of halloysite particles is not recommended to stabilize oil droplets in a Pickering emulsion, whereas a slightly flocculated state is more favorable (pH < 6).
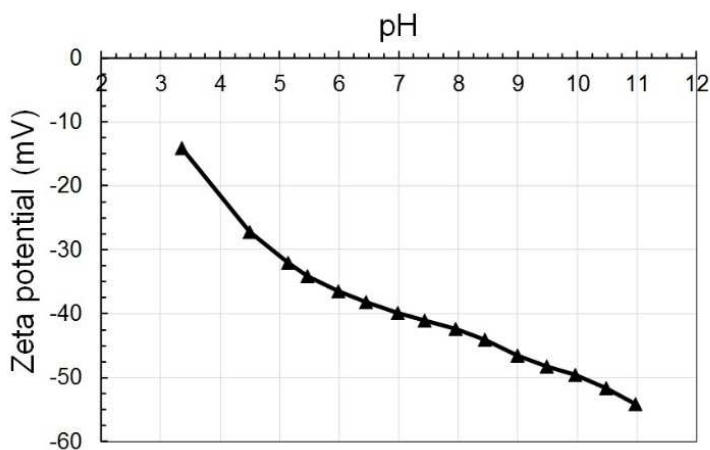
Figure 2: Zeta potential of an halloysite suspension as a function of the pH (volume fraction of halloysite 5.0 vol.% in deionized water, natural pH = 3.4)

(a)   (b)
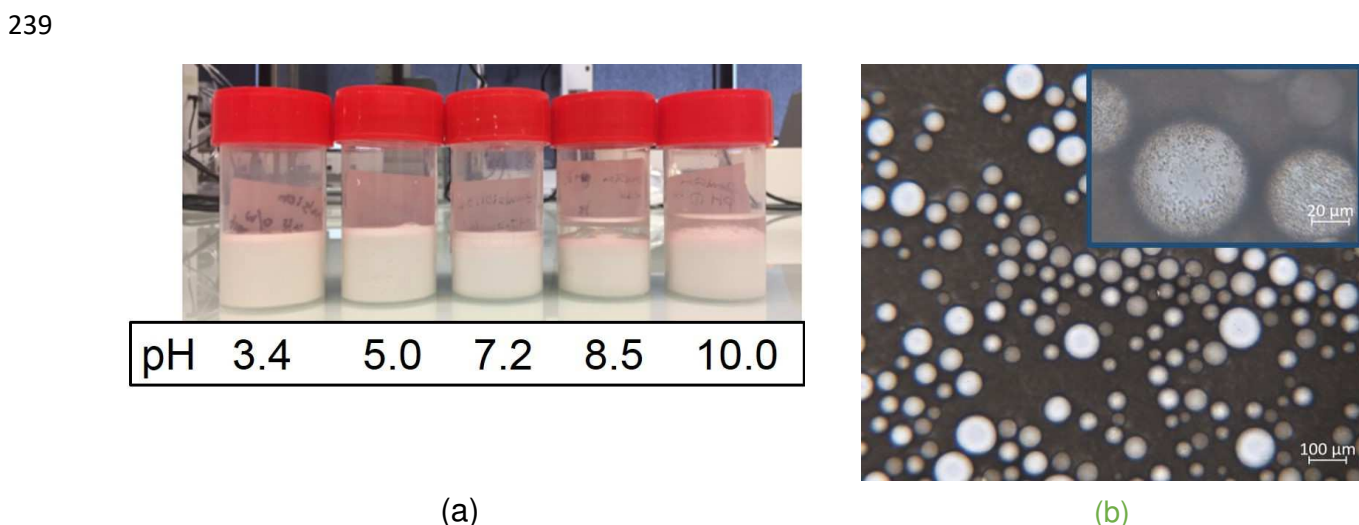
Figure 3: (a) Observations of the stability of Pickering emulsions prepared at different pH, after 1 week (volume fraction of halloysite 5.0 vol.% in deionized water, O/W ratio = 0.44 in volume), (b) O/W emulsion at pH 3.4

243

Oscillatory measurements have been conducted on relatively stable emulsions, at acidic pH
(from pH 3.4 to pH 6, Figure 4). The elastic (storage) modulus G' is always superior to the
viscous one (loss modulus) G'', corresponding to a solid-like behavior (Figure 5a). G' is the
largest for the case of natural pH. The critical strain increases with pH, whereas the cohesion
energy is similar regarding the large error bars (Figure 5b). Therefore the natural pH
corresponds to the most favorable pH to prepare a Pickering emulsion with halloysite.

250
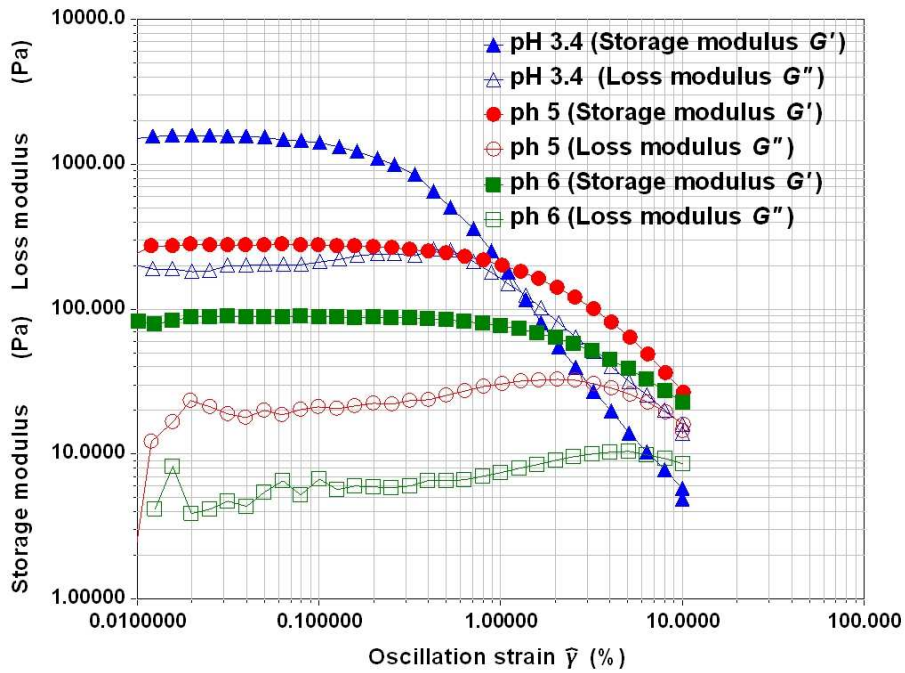
Figure 4: Oscillatory results for halloysite emulsions prepared at different pH

252
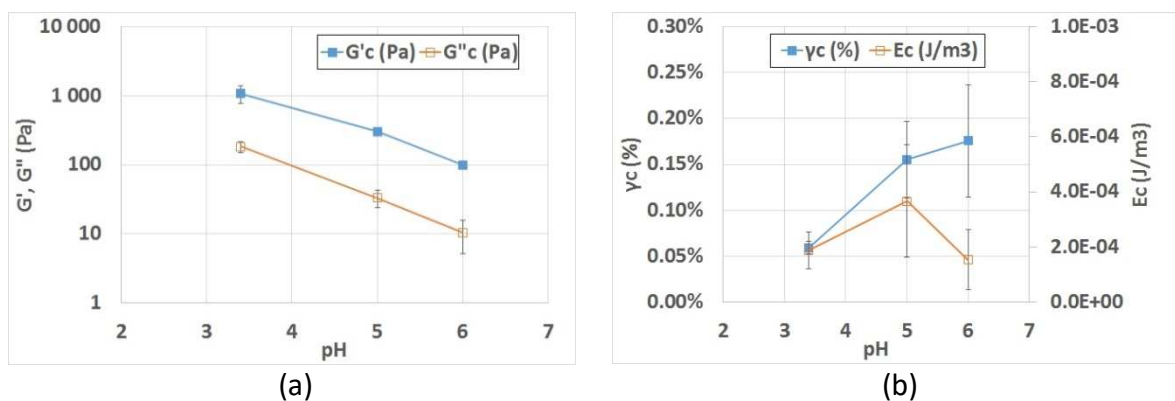
253 Figure 5: (a) critical storage modulus G'_c and critical loss modulus G''_c, (b) critical strain γ_c, and
254 cohesive energy E_c, of halloysite emulsions at different pH
255

256

257

3.2- Influence of NaCl concentration on halloysite suspensions and emulsions

Emulsions were prepared with NaCl at different concentrations to vary the ionic strength of halloysite suspensions. The conductivity evolution was significant, from 0.1 mS/cm without NaCl, to 1.3 mS/cm for [NaCl] = 0.01 M, and 9 mS/cm for [NaCl] = 0.1 M (Figure 6). However the stability of the emulsions was not influenced by NaCl concentration, and all emulsions were stable during several weeks, with no sedimentation neither coalescence nor creaming observed. From laser diffraction analysis (Figure 7), they all present a similar droplet size around 80 µm. The rheological behavior is also very similar whatever the NaCl concentration (Figures 8 and 9). The analysis of the oscillatory measurements gives a critical storage modulus G'_c comprised between 800 and 1000 Pa, and the critical loss modulus G''_c around 200 Pa. The critical deformation γ_c is around 0.06%, which leads to a relatively low cohesive energy around 0.15 mJ/m^3.

To explain this insensitivity, zeta potential was measured on halloysite suspensions by varying NaCl concentrations at a constant pH of 3.4 (natural pH). Zeta potential was also surprisingly quasi constant whatever NaCl concentration. It slightly decreased from -13 mV to -17 mV whereas the conductivity of the suspension increased drastically, from 0.1 to 9 mS/cm (Figure 6). In the DLVO theory, a higher conductivity usually leads to a compression of the double layer of the particles, leading to lower absolute values of zeta potential, and loss of stability. This is not observed here, with a low impact of NaCl concentration attributed to a low modification of particle-particle interactions in the suspension. This can be explained if Na$^+$ and Cl$^-$, which were assumed at first as non-potential determining ions, specifically adsorb on halloysite surfaces [42]. This is possible for halloysite particles, which present a very specific rolled plate morphology, with silica-like surface in the inner of the tubes, and alumina-like surface at the outer of the tubes [36][37][38], and therefore can adsorb both ions at acid pH.
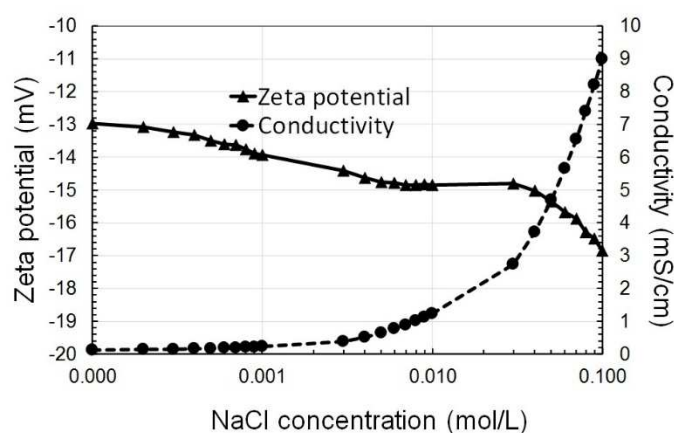
Figure 6: Evolution of zeta potential and conductivity of halloysite suspensions with NaCl concentrations varying from 0 to 0.1 M (volume fraction of halloysite 5.0 vol.%, natural pH = 3.4 - pH remains constant)
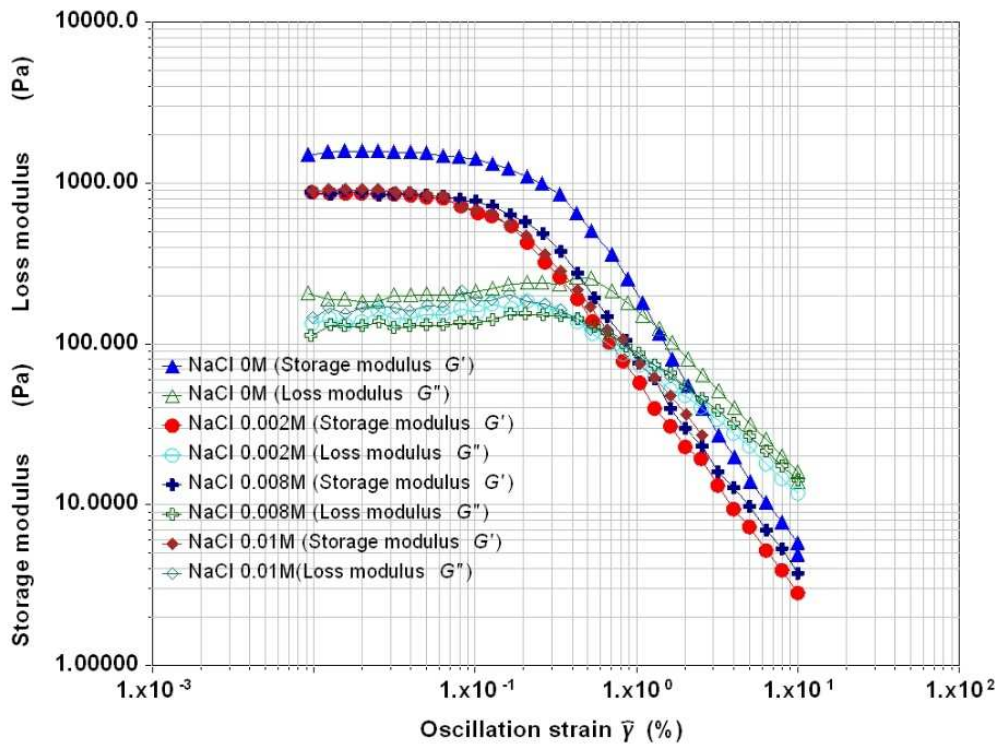
288
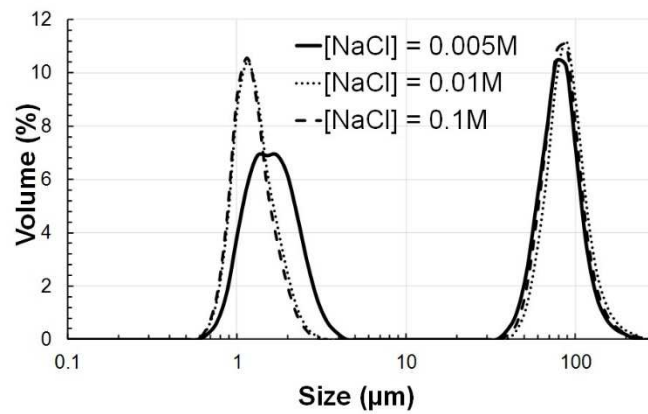
289

290 Figure 7: Laser diffraction analysis of halloysite emulsions at different NaCl concentrations and
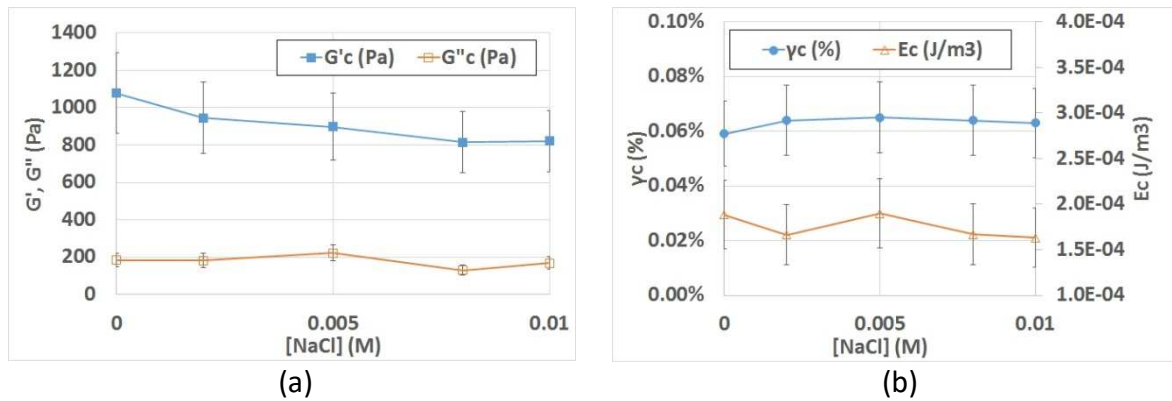291 natural pH

292

293

294 Figure 8: Oscillatory results G' and G'' for amplitude sweep at 1 Hz of halloysite emulsions at
295 different NaCl concentration and natural pH
296

297

(a)   (b)

Figure 9: (a) critical storage modulus G'$_c$ and critical loss modulus G''$_c$, (b) critical strain γ$_c$, and cohesive energy E$_c$, of halloysite emulsions at different NaCl concentration and natural pH

To conclude, these studies with different pH and NaCl concentrations are very informative as they highlight the predominant role of electrostatic interactions on the behavior of these emulsions. Their stability is improved if the dispersion of solid particles in the continuous phase is relatively limited, with medium zeta potential absolute values. Furthermore in this particular case, NaCl is not able to modify zeta potential and thus particle interactions, and emulsions present similar properties in terms of droplet size, stability, and rheology.

3.3- Influence of addition of binders (PVA and PEG) on halloysite suspensions and emulsions

Organics are usually added in ceramic processes in order to improve the processability or the handling of green pieces[43]. PVA and PEG were chosen respectively as a binder and a plasticizer for increasing the granule cohesion during freeze granulation.

At first the influence of PVA and PEG was studied in **halloysite suspensions**. Interfacial properties were investigated, because the lower the interfacial energy between two immiscible phases, the better it is for emulsification. Table 1 shows that adding halloysite particles at natural pH reduces drastically the interfacial energy compared to pure water, from 43 mN/m to 9 mN/m. This explains the stability of Pickering emulsions with halloysite, these particles alone are able to stabilize oil droplets. When adding PEG, the interfacial energy remains as low as with halloysite only. PVA addition increases the interfacial energy, and thus addition of both PVA and PEG leads to a similar value, around 15 mN/m. However this value remains low, and thus emulsification should be possible with PVA and PVA+PEG.

324   Table 1: Oil vs aqueous suspension interfacial energy (at natural pH)

	Interfacial energy (mN/m)
Oil/Water	43 ± 4
Oil/halloysite suspension (5.0 vol.%)	9 ± 2
Oil/halloysite suspension (5.0 vol.%) + PEG 1 wt.%	7 ± 2
Oil/halloysite suspension (5.0 vol.%) + PVA 1 wt.%	15 ± 2
Oil/halloysite suspension (5.0 vol.%) + PVA 1 wt.%+ PEG 1 wt.%	15 ± 2

325

326   The zeta potential of halloysite suspensions was measured with PEG, PVA and PEG+PVA, at

327   two pH values: natural pH of 3.4 corresponding to a zeta potential of halloysite suspension

328   around -14 mV (Figure 10a), and at pH 7.5 corresponding to a higher zeta potential absolute

329   value of halloysite suspension around -43 mV (Figure 10b). By adding PEG of low molecular

330   weight, zeta potential is relatively unmodified for the two pH, it attains -10 mV at natural pH,

331   and -41 mV at pH 7.5 for 1.5% of PEG. On the contrary, PVA strongly modifies the zeta

332   potential of the suspension, which increases at both pH, with a stronger evolution when the

333   initial value of the zeta potential is lower (at pH 7.5, Figure 11b). The strongest increase of the

334   zeta potential happens at the lowest binder ratio, for 0.2 % of PVA, and then zeta potential

335   increases slightly to attain -18 mV at 1.5% of PVA. PVA addition leads to a rapid screening of

336   the surface charge of halloysite, i.e. by pushing the shear plane (where the zeta potential is

337   measured) further from the particles surface. When polymers are adsorbed onto the particle

338   surface, changes in the ion distribution in the diffuse double layer will affect the absolute zeta

339   potential [44][45]. This is similar to cementitious systems where it has been shown that the

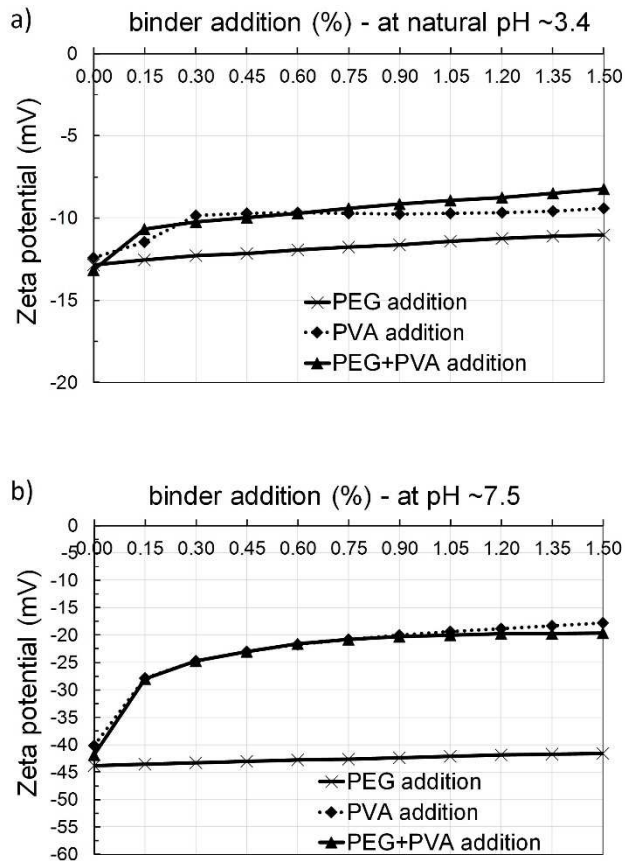340   adsorption of such polymeric layers give a significant steric contribution [46].

341

342

343

344

345

Figure 10: Effect of binder addition PVA, PEG and PVA+PEG on zeta potential of an halloysite suspension (concentration 5.0 vol.% in deionized water), a) at natural pH 3.4, and b) at pH 7.5

Then **halloysite emulsions** were prepared from a halloysite suspension at natural pH with different concentrations of PVA and PEG. These emulsions are composed of smaller droplets, between 10 and 30 µm in diameter whereas the mean droplet size was around 70 µm without additive as shown by laser diffraction analysis (Figure 11) and optical microscopy (Figure 12). The number of droplets is also more important, leading to less particles in the continuous phase. These polymers present an amphiphilic character which allow them to adsorb to halloysite surfaces via hydrogen bonding, and to increase as the same time the hydrophobicity of mineral particles thanks to their carbon chain, leading to a higher emulsification rate.
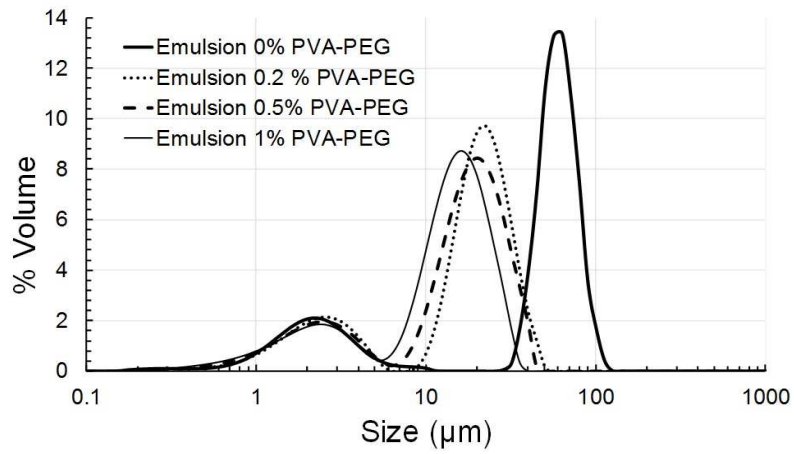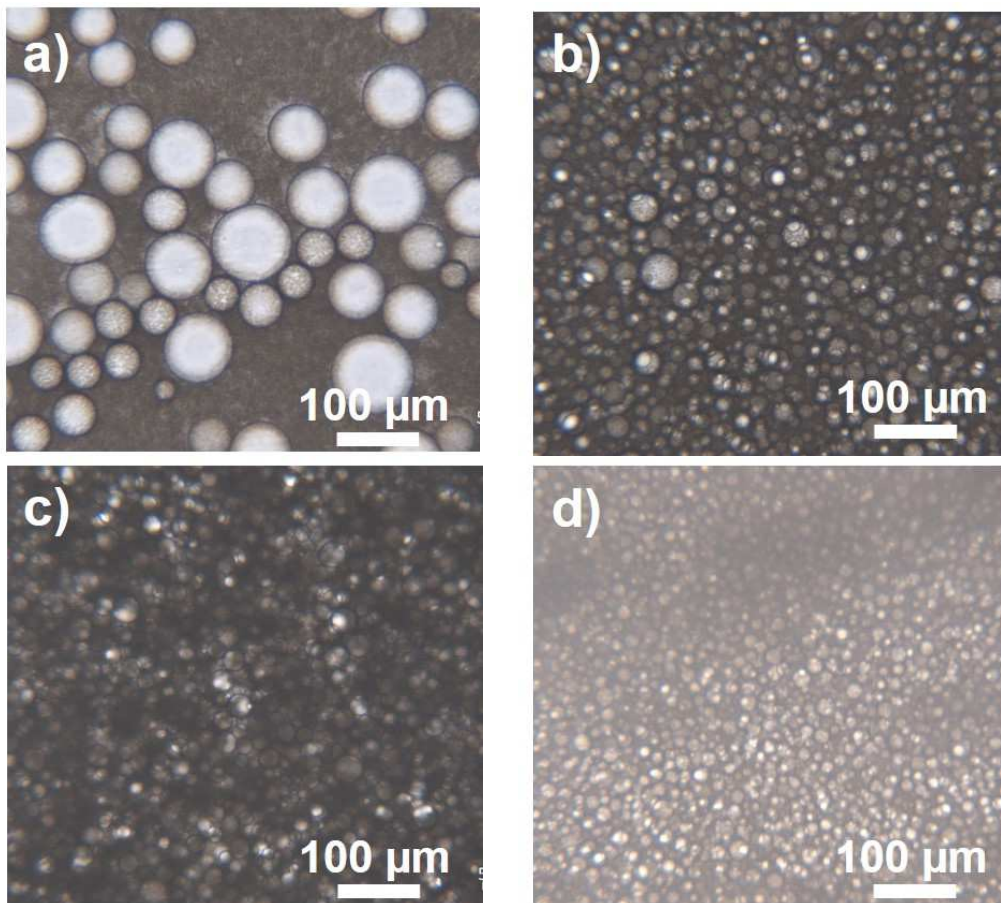
Figure 11: Laser diffraction analysis of halloysite emulsions from halloysite suspensions at natural pH with 0 – 0.2% - 0.5% - 1% PVA and PEG

Figure 12: Optical microscopy of halloysite emulsions at natural pH with a) 0% of PVA and PEG, b) 0,2% of PVA and PEG, c) 0,5% of PVA and PEG, d) 1% of PVA and PEG

365   Figure 13 shows steady state flow rheological experiments of halloysite emulsions with
366   different PVA+PEG concentrations. The addition of these organic binders decreases emulsion
367   viscosity. The emulsion without dispersant clearly presents a yield stress and a shear thinning
368   behavior, whereas the addition of binders decreases the yield stress and leads to a more
369   Newtonian flow. Besides, oscillatory measurements (Figure 14) show a very strong decrease
370   of the storage modulus G' by almost three orders of magnitude, as well as the loss modulus
371   G'', when adding 1 wt.% of PVA and PEG. Even if G' still remains higher than G'',
372   corresponding to a solid-like behavior, the emulsions prepared with binders are more fluid. At
373   the same time the critical strain increases with the concentration of binders, therefore these
374   emulsions support higher shear stresses. At the end they all present a similar value of their
375   cohesive energy around 0.5 mJ/m^3 considering the large error bars.
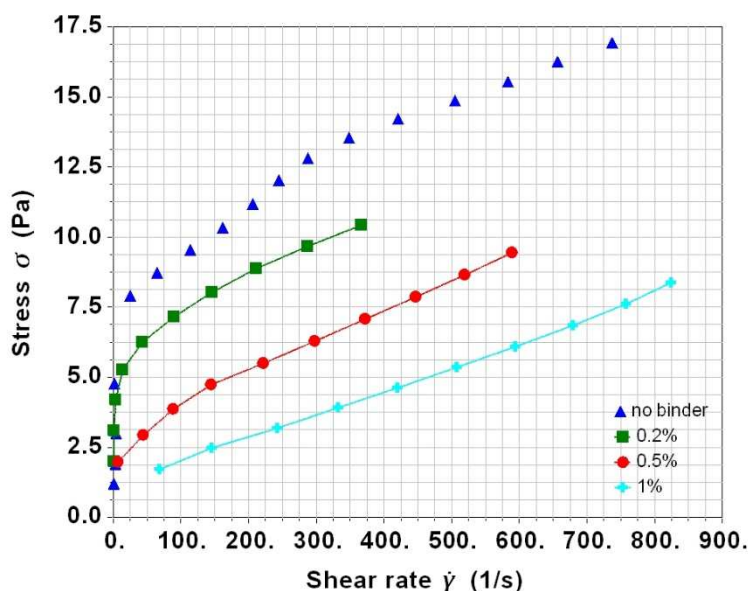
376

377   Figure 13: Steady state measurements for halloysite emulsions prepared at natural pH with
378   different concentrations of PVA and PEG
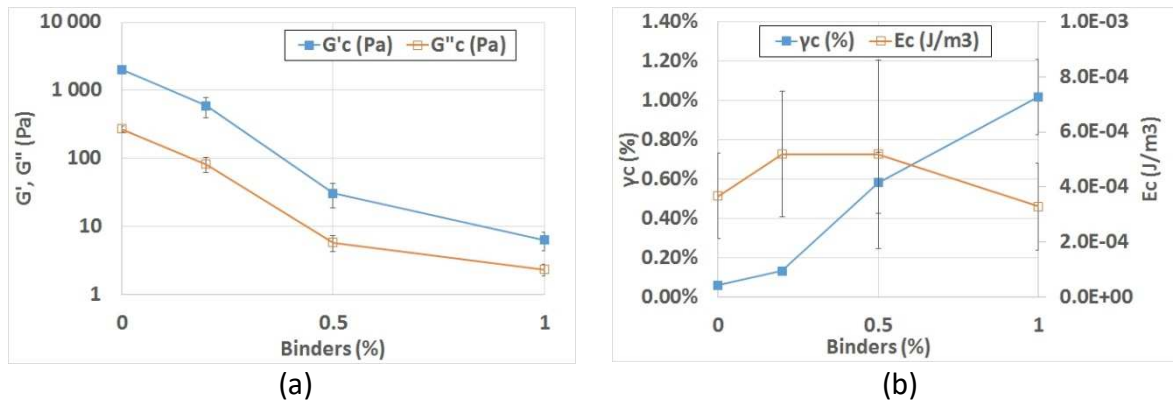
379
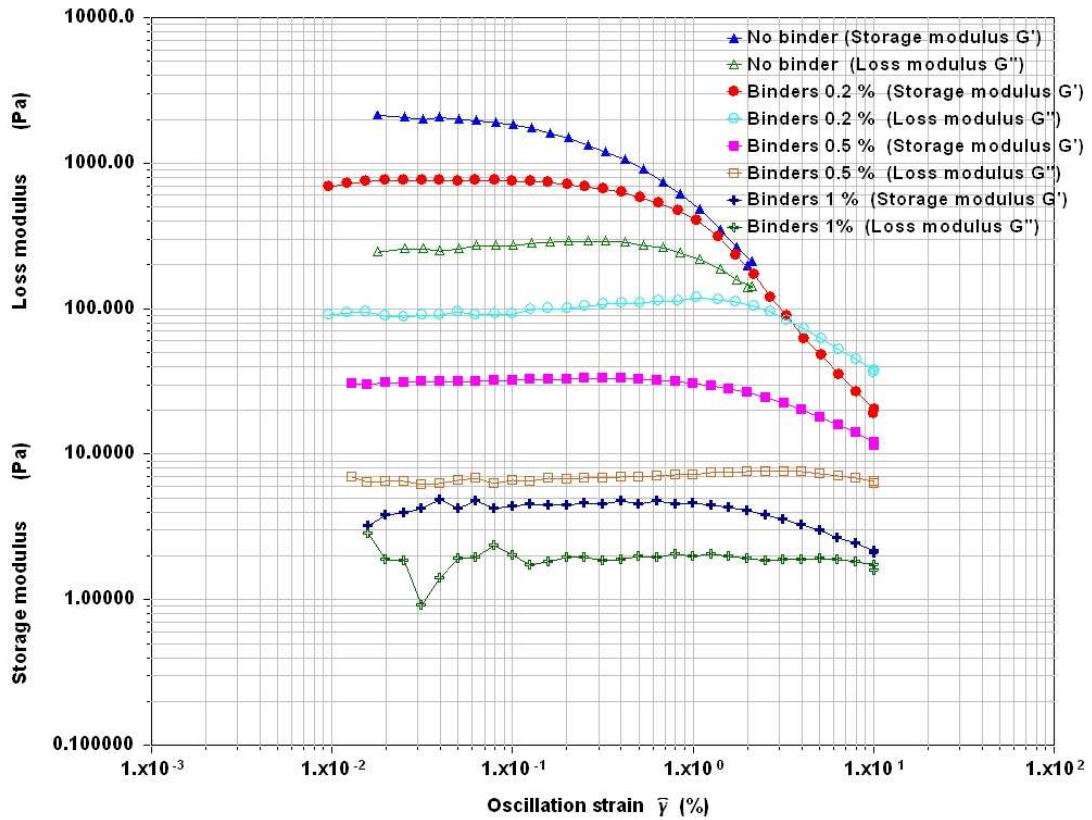
Figure 14: Oscillatory measurements for halloysite emulsions prepared at natural pH with different concentrations of PVA and PEG

382

| (a) | (b) |

383 Figure 15: (a) critical storage modulus G'$_c$ and critical loss modulus G"$_c$, (b) critical strain γ$_c$, and cohesive energy E$_c$, of halloysite emulsions at natural pH with different concentrations of PVA and PEG

386

387

388

3.4- Freeze granulation of emulsions and characterization of halloysite granules

The microstructure of powders obtained from freeze granulation of different Pickering emulsions stabilized with halloysite particles is studied below.

Besides their very different rheological behaviors, freeze granulation of emulsions prepared at different pH (pH 3.4, pH 5 and pH 6) led to granules with similar morphologies: some granules present a spherical shape as expected from the freeze granulation process, with diameters are comprised between 50 and 300 µm (Figure 16). Their cohesion is not good, as shown by the size distribution obtained on the dry granules. Indeed the size distribution is bimodal with a peak around 1 µm corresponding to halloysite particles, and another mode around 10 µm corresponding to aggregated particles and broken granules. They are very porous as shown by a closer observation of the surface, broken granules and also from an observation of the interior of granules, obtained from embedded granules in a resin after being cut and polished (Figure 16). These pictures exhibit a typical arrangement of halloysite particles, which form layers, certainly due to the fast freezing in liquid nitrogen, and the lyophilisation step. By comparing the microstructure of granules obtained from these different emulsions and from a halloysite suspension, there is no major difference: similar shape, diameter and porosity were obtained. Therefore we could conclude that Pickering emulsions were certainly broken during the spraying step. The dispersion of oil droplets was not retained during the process, and the porosity is mainly due to the relatively low solid fraction used for this process.

Freeze granulation of emulsions prepared at pH 3.4 with different concentrations of binders PVA + PEG led to the granules observed by SEM in Figure 18. All granules present spherical shape. The size distribution measured on dry granules increases with the concentration of PVA and PEG (Figure 17). The mode around 1 µm corresponding to halloysite particles has disappeared from 0.5% of binder, which corresponds to a higher cohesion of the granules. With the lowest binder concentrations (0.2 and 0.5 %), the surface morphology is close to what was observed without additive in Figure 16, i.e. a porous structure with layers of halloysite particles along freezing directions. However when increasing the binder concentration to 1%, the surface of granules looks smoother and the porosity is more homogeneously distributed. Contrary to emulsions without binders, typical columnar morphologies due to water elimination during the sublimation step are not observed. Inside granules some cavities are obtained which are attributed to the presence of oil droplets in the formulation. Therefore binder addition is necessary to retain the structure and give enough cohesion. This can be related to the lower viscosity of these emulsions, as well as their higher critical strain, which allow the conservation of their internal structure during the spraying step.

424

425

426

427
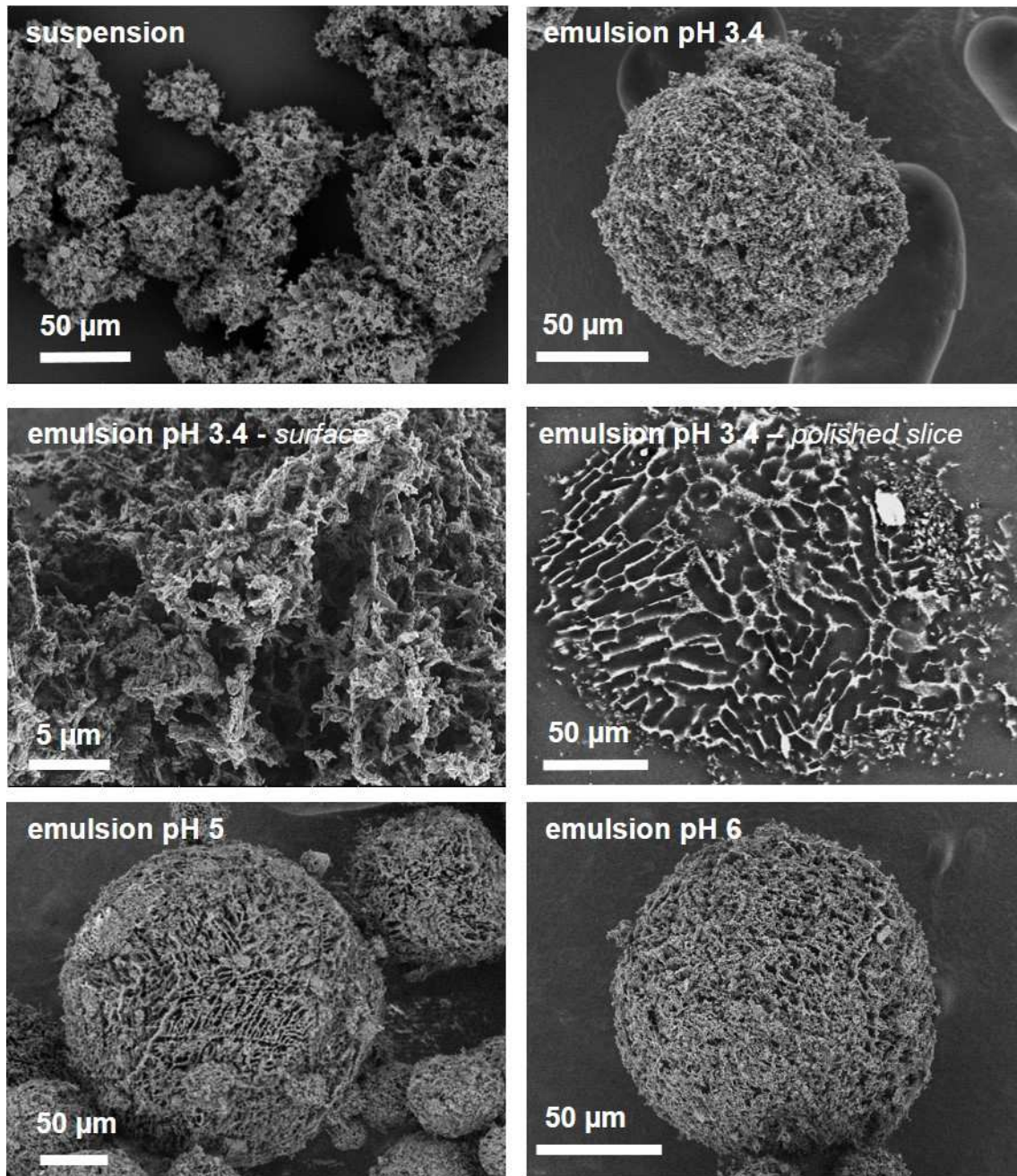
Figure 16: SEM observations of powders obtained by freeze granulation from halloysite
suspension and emulsions without binder
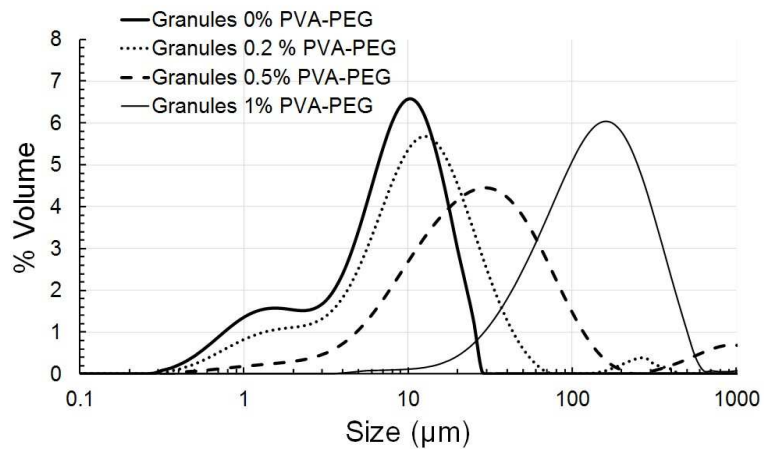
430

431　Figure 17: Laser diffraction analysis of granules obtained by freeze granulation of halloysite
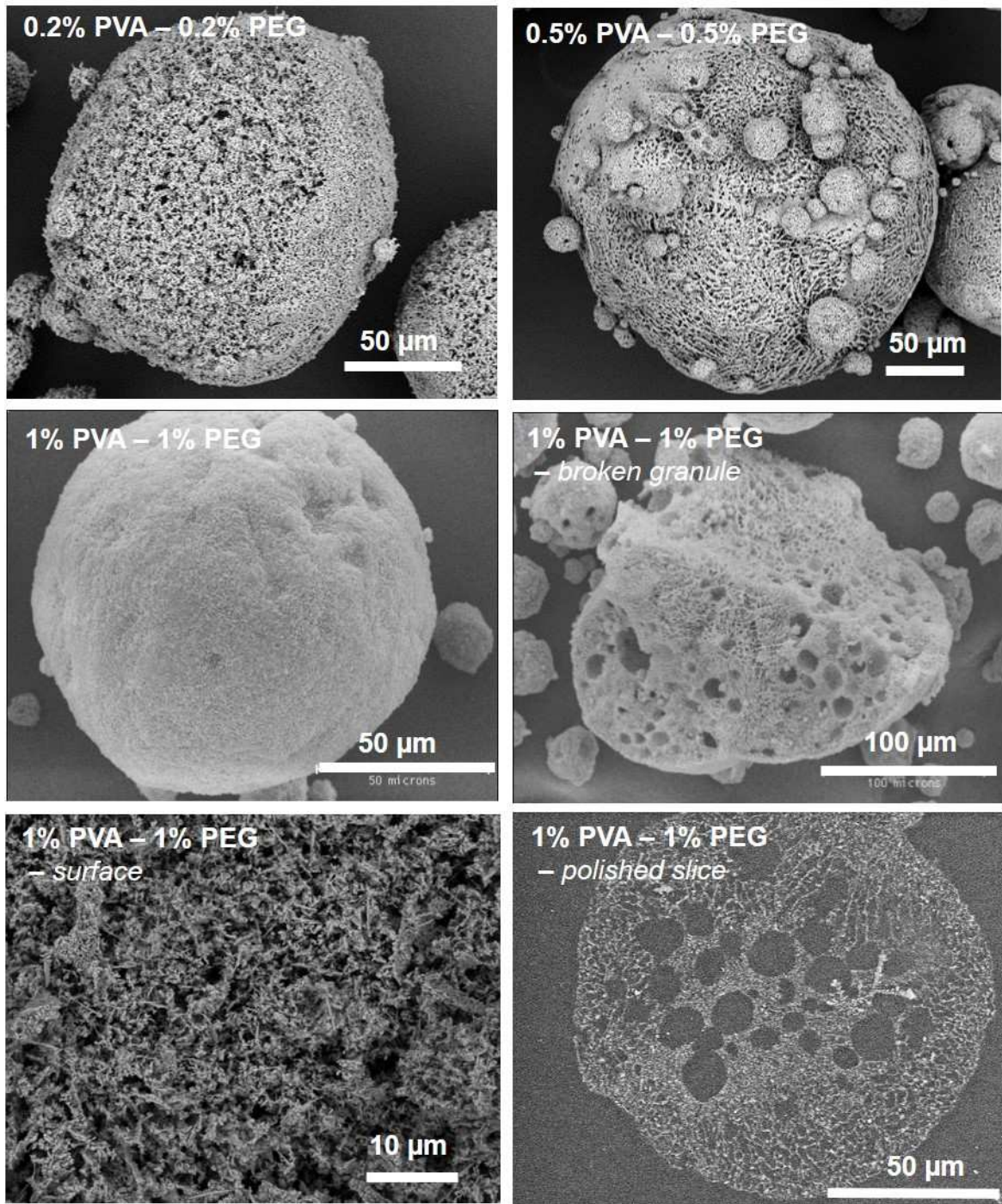
432　emulsions at natural pH with 0 – 0.2% - 0.5% - 1% PVA and PEG

Figure 18: SEM observations of powders obtained by freeze granulation from halloysite emulsions with different concentrations of PVA and PEG

4- Conclusion

Freeze granulation was applied to Pickering emulsions to prepare porous granules. Halloysite was chosen on the basis of a former study which has shown halloysite can give stable Pickering emulsions at a relatively high solid fraction, with an interesting rheological behavior and a high cohesion. From a fundamental approach, one of the main interesting result from this study is the exhibition of the strong influence of electrostatic interactions on emulsion stability, varying the pH and NaCl concentration. In classical Pickering systems hydrophobic effects have to be considered, which is not the case with a stabilization of O/W emulsions by clays only. The addition of organic additives led also to stable emulsions, and more importantly to freeze-dried granules which preserved the emulsion shape. By studying their rheological behavior, these emulsions showed the lowest viscosity, and the highest critical strain. Therefore they were able to support higher shear stresses, necessary during the spraying step. Therefore Pickering emulsions stabilized with clays such as halloysite present very good performances. These materials are also readily available, cheap and natural resources. They offer a great opportunity for the development of surfactant-free emulsions that can be used in large markets such as cosmetics and food products. Moreover by freeze granulation of Pickering emulsions, porous halloysite granules were obtained, which have a high potential for the encapsulation of organic substances, or as catalyst supports.

References

[1] Y. Chevalier and M.-A. Bolzinger, "Emulsions stabilized with solid nanoparticles: Pickering emulsions," *Colloids Surf. Physicochem. Eng. Asp.*, vol. 439, pp. 23–34, 2013.

[2] W. Ramsden, "Separation of Solids in the Surface-Layers of Solutions and 'Suspensions' (Observations on Surface-Membranes, Bubbles, Emulsions, and Mechanical Coagulation). – Preliminary Account," *Proc. R. Soc. Lond.*, vol. 72, no. 477–486, pp. 156–164, Jan. 1903.

[3] S. U. Pickering, "CXCVI.—Emulsions," *J. Chem. Soc. Trans.*, vol. 91, no. 0, pp. 2001–2021, Jan. 1907.

[4] V. B. Menon and D. T. Wasan, "Characterization of oil—water interfaces containing finely divided solids with applications to the coalescence of water-in-oil Emulsions: A review," *Colloids Surf.*, vol. 29, no. 1, pp. 7–27, 1988.

[5] B. P. Binks, "Particles as surfactants—similarities and differences," *Curr. Opin. Colloid Interface Sci.*, vol. 7, no. 1–2, pp. 21–41, Mar. 2002.

476 [6] B. P. Binks and J. H. Clint, "Solid Wettability from Surface Energy Components: Relevance to
477   Pickering Emulsions," *Langmuir*, vol. 18, no. 4, pp. 1270–1273, 2002.
478 [7] R. Aveyard, B. P. Binks, and J. H. Clint, "Emulsions stabilised solely by colloidal particles," *Adv.*
479   *Colloid Interface Sci.*, vol. 100–102, pp. 503–546, 2003.
480 [8] B. P. Binks and S. O. Lumsdon, "Influence of Particle Wettability on the Type and Stability of
481   Surfactant-Free Emulsions†," *Langmuir*, vol. 16, no. 23, pp. 8622–8631, Nov. 2000.
482 [9] G. Lagaly, M. Reese, and S. Abend, "Smectites as colloidal stabilizers of emulsions: I.
483   Preparation and properties of emulsions with smectites and nonionic surfactants," *Appl. Clay*
484   *Sci.*, vol. 14, no. 1–3, pp. 83–103, 1999.
485 [10] S. Arditty, V. Schmitt, J. Giermanska-Kahn, and F. Leal-Calderon, "Materials based on solid-
486   stabilized emulsions," *J. Colloid Interface Sci.*, vol. 275, no. 2, pp. 659–664, 2004.
487 [11] K. Lebdioua, A. Aimable, M. Cerbelaud, A. Videcoq, and C. Peyratout, "Influence of different
488   surfactants on Pickering emulsions stabilized by submicronic silica particles," *J. Colloid Interface*
489   *Sci.*, vol. 520, pp. 127–133, Jun. 2018.
490 [12] B. P. Binks, W. Liu, and J. A. Rodrigues, "Novel Stabilization of Emulsions via the
491   Heteroaggregation of Nanoparticles," *Langmuir*, vol. 24, no. 9, pp. 4443–4446, May 2008.
492 [13] M. Cerbelaud, A. Aimable, and A. Videcoq, "Role of Electrostatic Interactions in Oil-in-Water
493   Emulsions Stabilized by Heteroaggregation: An Experimental and Simulation Study," *Langmuir*,
494   vol. 34, no. 51, pp. 15795–15803, Dec. 2018.
495 [14] S. Abend, N. Bonnke, U. Gutschner, and G. Lagaly, "Stabilization of emulsions by
496   heterocoagulation of clay minerals and layered double hydroxides," *Colloid Polym. Sci.*, vol.
497   276, no. 8, pp. 730–737, Sep. 1998.
498 [15] Y. Nonomura and N. Kobayashi, "Phase inversion of the Pickering emulsions stabilized by plate-
499   shaped clay particles," *J. Colloid Interface Sci.*, vol. 330, no. 2, pp. 463–466, 2009.
500 [16] G. Lagaly, M. Reese, and S. Abend, "Smectites as colloidal stabilizers of emulsions: II.
501   Rheological properties of smectite-laden emulsions," *Appl. Clay Sci.*, vol. 14, no. 5–6, pp. 279–
502   298, 1999.
503 [17] N. P. Ashby and B. P. Binks, "Pickering emulsions stabilised by Laponite clay particles," *Phys.*
504   *Chem. Chem. Phys.*, vol. 2, no. 24, pp. 5640–5646, 2000.
505 [18] B. Rotenberg, "Modélisation multi-échelles du comportement de l'eau et des ions dans les
506   argiles," PhD Thesis, Université Pierre et Marie Curie - Paris VI, 2007.
507 [19] D. Kpogbemabou, G. Lecomte-Nana, A. Aimable, M. Bienia, V. Niknam, and C. Carrion, "Oil-in-
508   water Pickering emulsions stabilized by phyllosilicates at high solid content," *Colloids Surf.*
509   *Physicochem. Eng. Asp.*, vol. 463, pp. 85–92, 2014.
510 [20] K. Rundgren, O. Lyckfeldt, and M. Sjostedt, "Improving Powders With Freeze Granulation,"
511   *Ceramic Industry*, vol. 153, pp. 40–44, 2003.
512 [21] W. J. J. Walker, J. S. Reed, and S. K. Verma, "Influence of Slurry Parameters on the
513   Characteristics of Spray-Dried Granules," *J. Am. Ceram. Soc.*, vol. 82, no. 7, pp. 1711–1719,
514   1999.
515 [22] E. Lintingre, F. Lequeux, L. Talini, and N. Tsapis, "Control of particle morphology in the spray
516   drying of colloidal suspensions," *Soft Matter*, vol. 12, no. 36, pp. 7435–7444, Sep. 2016.
517 [23] S. Shanmugam, "Granulation techniques and technologies: recent progresses," *BioImpacts*, vol.
518   5, no. 1, pp. 55–63, Aug. 2017.
519 [24] M. Stuer, Z. Zhao, and P. Bowen, "Freeze granulation: Powder processing for transparent
520   alumina applications," *J. Eur. Ceram. Soc.*, vol. 32, no. 11, pp. 2899–2908, Aug. 2012.
521 [25] M. Stuer and P. Bowen, "Yield stress modelling of doped alumina suspensions for applications
522   in freeze granulation: towards dry pressed transparent ceramics," *Adv. Appl. Ceram.*, vol. 111,
523   no. 5–6, pp. 254–261, Aug. 2012.
524 [26] F. La Lumia, L. Ramond, C. Pagnoux, and G. Bernard-Granger, "Fabrication of homogenous
525   pellets by freeze granulation of optimized TiO2-Y2O3 suspensions," *J. Eur. Ceram. Soc.*, vol. 39,
526   no. 6, pp. 2168–2178, Jun. 2019.

527 [27] O. Lyckfeldt, K. Rundgren, and M. Sjöstedt, "Freeze Granulation for the Processing of Silicon
528   Nitride Ceramics," *Key Eng. Mater.*, 2004.
529 [28] Q. Wang, S. M. Olhero, J. M. F. Ferreira, W. Cui, K. Chen, and Z. Xie, "Hydrolysis Control of AlN
530   Powders for the Aqueous Processing of Spherical AlN Granules," *J. Am. Ceram. Soc.*, vol. 96, no.
531   5, pp. 1383–1389, 2013.
532 [29] P. Barick, B. P. Saha, S. V. Joshi, and R. Mitra, "Spray-freeze-dried nanosized silicon carbide
533   containing granules: Properties, compaction behaviour and sintering," *J. Eur. Ceram. Soc.*, vol.
534   36, no. 16, pp. 3863–3877, Dec. 2016.
535 [30] A. R. Studart, U. T. Gonzenbach, E. Tervoort, and L. J. Gauckler, "Processing Routes to
536   Macroporous Ceramics: A Review," *J. Am. Ceram. Soc.*, vol. 89, no. 6, pp. 1771–1789, 2006.
537 [31] I. Akartuna, A. R. Studart, E. Tervoort, and L. J. Gauckler, "Macroporous Ceramics from Particle-
538   stabilized Emulsions," *Adv. Mater.*, vol. 20, no. 24, pp. 4714–4718, 2008.
539 [32] I. Lesov, S. Tcholakova, M. Kovadjieva, T. Saison, M. Lamblet, and N. Denkov, "Role of Pickering
540   stabilization and bulk gelation for the preparation and properties of solid silica foams," *J.
541   Colloid Interface Sci.*, vol. 504, pp. 48–57, Oct. 2017.
542 [33] J. A. Lewis, J. E. Smay, J. Stuecker, and J. Cesarano, "Direct Ink Writing of Three-Dimensional
543   Ceramic Structures," *J. Am. Ceram. Soc.*, vol. 89, no. 12, pp. 3599–3609, 2006.
544 [34] M. A. Torres Arango, N. J. Morris, and K. A. Sierros, "Direct Writing and Controlling of
545   Hierarchical Functional Metal-Oxides: Bio-inspired Multiphase Processing, 3D Printing and
546   Hierarchical Cellular Structuring," *JOM*, vol. 70, no. 9, pp. 1823–1829, 2018.
547 [35] L. Alison *et al.*, "3D printing of sacrificial templates into hierarchical porous materials," *Sci. Rep.*,
548   vol. 9, no. 1, 2019.
549 [36] R. Kamble, M. Ghag, S. Gaikawad, and B. K. Panda, "Halloysite Nanotubes and Applications: A
550   Review," *J. Adv. Sci. Res.*, vol. 3, no. 2, pp. 25–29, 2012.
551 [37] P. Yuan, D. Tan, and F. Annabi-Bergaya, "Properties and applications of halloysite nanotubes:
552   Recent research advances and future prospects," *Appl. Clay Sci.*, vol. 112–113, pp. 75–93, 2015.
553 [38] G. Lazzara *et al.*, "An assembly of organic-inorganic composites using halloysite clay
554   nanotubes," *Curr. Opin. Colloid Interface Sci.*, vol. 35, pp. 42–50, 2018.
555 [39] N. Gabas, N. Hiquily, and C. Laguérie, "Response of Laser Diffraction Particle Sizer to
556   Anisometric Particles," *Part. Part. Syst. Charact.*, vol. 11, no. 2, pp. 121–126, 1994.
557 [40] E. Chibowski, A. E. Wiacek, L. Holysz, and K. Terpilowski, "Investigation of the Electrokinetic
558   Properties of Paraffin Suspension. 1. In Inorganic Electrolyte Solutions," *Langmuir*, vol. 21, no.
559   10, pp. 4347–4355, May 2005.
560 [41] M. Cerbelaud, A. Videcoq, L. Alison, E. Tervoort, and A. R. Studart, "Early Dynamics and
561   Stabilization Mechanisms of Oil-in-Water Emulsions Containing Colloidal Particles Modified
562   with Short Amphiphiles: A Numerical Study," *Langmuir*, vol. 33, no. 50, pp. 14347–14357, Dec.
563   2017.
564 [42] M. Donnet, P. Bowen, and J. Lemaiˆtre, "A thermodynamic solution model for calcium
565   carbonate: Towards an understanding of multi-equilibria precipitation pathways," *J. Colloid
566   Interface Sci.*, vol. 340, no. 2, pp. 218–224, Dec. 2009.
567 [43] J. S. Reed, *Principles of Ceramics Processing*. Wiley, 1995.
568 [44] A. U. Khan, B. J. Briscoe, and P. F. Luckham, "Interaction of binders with dispersant stabilised
569   alumina suspensions," *Colloids Surf. Physicochem. Eng. Asp.*, vol. 161, no. 2, pp. 243–257, Jan.
570   2000.
571 [45] J. Ma, R. Zhang, C. H. Liang, and L. Weng, "Colloidal characterization and electrophoretic
572   deposition of PZT," *Mater. Lett.*, vol. 57, no. 30, pp. 4648–4654, Dec. 2003.
573 [46] M. Palacios *et al.*, "Repulsion forces of superplasticizers on ground granulated blast furnace slag
574   in alkaline media, from AFM measurements to rheological properties," *Mater. Construccion*,
575   vol. 62, no. 308, pp. 489–513, 2012.
576